A Discussion of the Molecular Mechanisms of Moisture Transport in Epoxy Resins

CHRISTOPHER L. SOLES,* ALBERT F. YEE

Department of Materials Science & Engineering, University of Michigan, Ann Arbor, Michigan 48109-2136

Received 24 February 1999; revised 13 September 1999; accepted 13 December 1999

ABSTRACT: A typical epoxy formulation can absorb several weight percent of water, seriously degrading the physical properties of the resin. In two preceding publications (Soles, C. L.; Chang, F. T.; Bolan, B. A.; Hristov, H. A.; Gidley, D. W.; Yee, A. F. J Polym Sci Part B: Polym Phys 1998, 36, 3035; Soles, C. L.; Chang, F. T.; Gidley, D. W.; Yee, A. F. J Polym Sci Part B: Polym Phys 2000, 38, 776), the role of electron density heterogeneities, or nanovoids (as measured through positron annihilation lifetime spectroscopy), in the moisture-transport process is elucidated. In this article, the influence of these nanovoids is examined in light of both the specific epoxy–water interactions and the molecular motions of the glassy state to develop a plausible picture of the moisture-transport process in an amine-cured epoxy resin. In this description, the topology (nanopores), polarity, and molecular motions act in concert to control transport. Water traverses the epoxy through the network of nanopores, which are also coincident with the polar hydroxyls and amines. In this respect, the nanopores provide access to the polar interaction sites. Furthermore, the sub-T_g (glass-transition temperature) molecular motions coincident with the onset of the β-relaxation process incorporate these polar sites and, hence, regulate the association of water with the epoxy. In effect, the kinetics of the transport mirror the dynamics associated with the local-scale motions of the β-relaxation process, and this appears to be the rate-limiting factor in transport. The volume fraction of the nanopores does not appear to be rate-limiting in the case of an amine-cured epoxy, contrary to popular theories of transport. © 2000 John Wiley & Sons, Inc. J Polym Sci B: Polym Phys 38: 792–802, 2000

Keywords: moisture; transport; diffusion; absorption; positron annihilation lifetime spectroscopy; epoxy; polymer

INTRODUCTION

Epoxies comprise a class of polymeric materials that are technically relevant to modern society. For example, epoxy-based composites are widely used in structural applications, such as airframe materials in the aerospace industry. Approximately 60% of the external surface area, or 19% of the total weight, of the Navy's F/A-18 E/F aircraft consists of an epoxy–carbon-fiber composite.[1] Similarly, epoxies are widely used in the microelectronics industry as the workhorse encapsulant and underfill agent in the mounting of chip assemblies to the printed circuit board. Furthermore, the printed circuit board itself is generally an epoxy/glass-fiber composite. Epoxies clearly constitute a class of polymeric materials that are of significant technical relevance.

However, in most applications the epoxy-based component has the potential of being exposed to moist conditions or a humid environment. This can lead to problems because most epoxies absorb between 1 and 7 wt % moisture. Absorbed mois-

Correspondence to: A. F. Yee (E-mail: afyee@engin.umich.edu)

* *Present address:* NIST, 100 Bureau Drive, Gaithersburg, MD, 20899-8541

Journal of Polymer Science: Part B: Polymer Physics, Vol. 38, 792–802 (2000)

ture has deleterious effects on the physical properties of epoxies and can, therefore, greatly compromise the performance of an epoxy-based component. To sufficiently address this problem, researchers need to understand the molecular details of the moisture-transport process.

In this article, we discuss the interrelated nature of the crucial molecular aspects of moisture transport in amine-cured epoxy resins. This discussion is the culmination of two previous publications[2,3] in which the roles of network topology in the transport process are explored. The same epoxies are discussed in this article, so the reader is referred to the previous two articles for the sample identifications and descriptions. In the first of these two articles,[2] the epoxy topology is quantified via positron annihilation lifetime spectroscopy (PALS) in terms of the size and volume fraction of nanometer-sized pores. Then, the role of these nanopores in establishing the equilibrium moisture uptake is examined. The latter publication[3] extends these ideas and explores how the nanopores affect the kinetics of moisture transport. Together, these works provide a detailed understanding of how the nanopores influence the entire transport process. In this article, the combined effects of the nanopores, specific epoxy–water interactions, and molecular motions are discussed to provide a reasonable molecular description of the moisture-transport mechanisms in an amine-cured epoxy.

CORRELATIONS BETWEEN TOPOLOGY AND TRANSPORT

Before proceeding further, we briefly summarize the salient findings of the previous two articles in which topology is correlated to both ultimate moisture uptake[2] and the kinetics of transport.[3] As mentioned previously, the PALS technique is capable of measuring both the size and number of nanovoids. The product of these quantities defines the volume fraction of the nanopores, $V_h(T)$, which is determined as a function of temperature, as demonstrated in Figure 2 of the original publication.[2] Extrapolating the low-temperature portion of this plot to absolute zero identifies the intrinsic hole volume fraction, V_0. V_0 represents those nanopores inherent to a glassy polymer that cannot be cooled from the system. As the temperature is raised, additional unoccupied volume is created from thermal expansion and vibrations. This dynamic contribution is defined as $V_d(T)$, and at any temperature, $V_h(T)$ is the sum of V_0 and $V_d(T)$. For the epoxies examined here, a simplified spherical nanopore model is employed to estimate that the typical nanopores range from 5.0 to 6.1 Å in diameter with a $V_h(T)$ that accounts for approximately 3 to 7 vol % of the material. The intrinsic fraction V_0 is typically one-fifth to three-fifths of the total volume fraction, with the extremes occurring in the low crosslink density (flexible) and high crosslink density (rigid) resins, respectively.

Considering moisture absorption, a larger intrinsic hole volume leads to an increased moisture uptake within a series of resins with similar polarity (where topology is altered through diamine/monoamine substitutions). This dependence on V_0 is greatest at 5 °C and diminishes with temperature. Although V_0 has a notable influence on uptake, polarity is of primary importance: highly polar resins absorb more water than less polar ones. For this reason, a unique and absolute correlation between uptake and V_0 is not observed. Only within resins of comparable polarity does V_0 correlate with uptake. Furthermore, V_0 is intimately tied to the effective polarity of the resin. The intrinsic hole volume elements are localized at the crosslink junctions, which are also the locations of the polar hydroxyls and amines. The effect of V_0 is to open the matrix and reveal polar sites, thus enhancing the ability of water to access the interaction sites.

Although the uptake readily correlates to topology, a strong correlation is not observed with respect to the kinetics of transport. At 5 and 35 °C, the diffusion coefficient (D) increases slightly with the average size or volume of the nanopores, showing a mild, positive exponential dependence. Above 35 °C, D is independent of the size of the nanopores, described more appropriately by an exponent of zero. At all temperatures, D exhibits a similar independence on the volume fractions of nanopores. Such behavior is observed with all of the resins except the non-amine series. In these resins, the lack of polar sites significantly enhances diffusion. At 5 °C, D in the non-amine resins is one order of magnitude greater than any of the amine-containing resins. However, this difference diminishes with temperature and at 90 °C, all diffusion coefficients are within experimental error.

If the comparison between kinetics and topology is limited to the initial stages of uptake, the initial absorption rate does increase with the intrinsic hole volume fraction. This initial absorp-

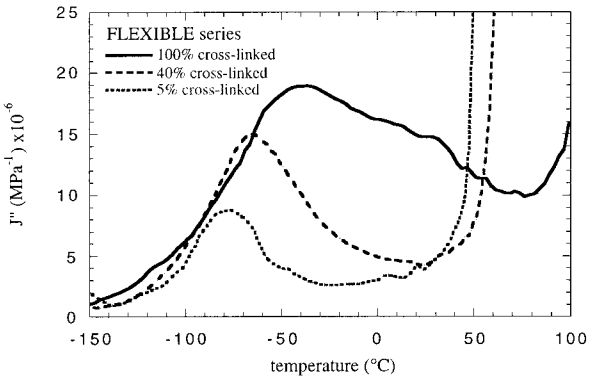

Figure 1. The loss compliance as a function of temperature for a frequency of 1 Hz in β-relaxation spectra of the flexible resins. As the crosslink density is reduced, the breadth and height of the peak are reduced, whereas the onset remains unchanged. Reprinted from Polymer, 38, Heux, L.; Halary, J.-L.; Lauprêtre, F.; Monnerie, L. Dynamic Mechanical and ^{13}C NMR Investigations of the Molecular Motions Involved in the β Relaxation of Epoxy Networks Based on DGEBA and Aliphatic Amines, p. 1767, Copyright 1997, with permission from Elsevier Science.

tion rate has as its units mg H_20/cm^2 $min^{1/2}$ and represents the number of water molecules entering the sample per unit area per unit of time (analogous to flux). Although the diffusion measurements take anywhere from several days to months to complete, the initial absorption rate measurements occur within the first 15 to 30 min. The failure of the long-term kinetics to correlate with the topology, as quantified in the dry state, may be evidence of water being able to alter the topology. Only in the initial stages of absorption is the dry topology relevant to the transport behavior.

DISCUSSION

Influence of Molecular Motions

Sub-T_g (glass-transition temperature) molecular motions have long been reported to influence the transport process in polymer-penetrant systems.[4] Of interest here, the labs of Halary and Monnerie[5–9] have generated extensive dynamic mechanical data on the rigid, semirigid, and flexible resins. Figure 1, reproduced from one of their publications,[8] typifies the response of the dynamic mechanical spectra to changes in topology achieved by decreasing crosslink density via diamine/monoamine substitutions. The fully crosslinked material exhibits a broad β-relaxation peak commencing at -100 °C at a frequency of 1 Hz. As the crosslink density is reduced, the onset, or low-temperature portion of the peak, is invariable, whereas the peak breadth, position, and height are diminished. Although Figure 1 is for flexible resins, an analogous behavior has been observed with semirigid and rigid resins.[6,8] In fact, virtually all epoxies exhibit identical β-relaxation behaviors in the onset region, regardless of the architecture of the epoxy or curing agent; this similarity has been noted by several authors.[8–15]

Although a precise understanding of the molecular mechanisms responsible for the β-relaxation mechanism remains elusive, several truisms are noted. It is generally accepted that the primary, or most fundamental, motions responsible for the relaxation are activated at the onset of the relaxation, whereas the peak breadth and height depend on the cooperativity or extent of the motions.[8,16–18] In a heavily crosslinked epoxy, the dense covalent network constitutes a highly coupled system, and one must go to high temperatures to entirely activate the relaxation mechanisms. As the crosslink density is diminished, decoupling allows full activation at a lower temperature because of the curtailed extent of the relaxation. In terms of normal-mode analysis, the high-frequency local modes are activated in the onset regime of the relaxation, regardless of the crosslink density. In the high crosslink density resins, covalent coupling enables large-scale, low-frequency modes. The greater density of states from these higher order modes requires greater thermal energy to attain full activation, extending the relaxation peak on the high-temperature side. The resulting relaxation in these highly cooperative networks should be very complex. This is evidenced by the failure of time–temperature superposition in highly crosslinked resins;[8] the relaxation is thermorheologically complex. In contrast, the low crosslink density resins exhibit a relatively simple β relaxation that adequately conforms to time–temperature superposition;[8] the relaxation appears thermorheologically simple.

This discussion emphasizes the similarities of local-scale motions in the β relaxation for nearly all epoxies. In a strikingly similar fashion, the diffusion coefficients exhibit insignificant variation with the extent or cooperativity of the β relaxation. Both the diffusion coefficient of water and the β-relaxation onset appear independent of topology. This implies that the absorbed moisture is only sensitive to the isolated, local motions and cannot feel the larger scale motions occurring be-

Table I. Activation Energies for Both the Diffusion Coefficient and the β-Relaxation Process as Determined by Dynamic Mechanical Analysis (DMA)

Sample	Diffusion	% Crosslink	DMA Peak[a]	DMA Onset[a]
Rigid resins				
100% crosslinked	46 kJ/mol	100%	75 kJ/mol	33 kJ/mol
80% crosslinked	45 kJ/mol	75%	58 kJ/mol	32 kJ/mol
60% crosslinked	43 kJ/mol	0%	53 kJ/mol	28 kJ/mol
40% crosslinked	43 kJ/mol			
Semirigid resins				
100% crosslinked	42 kJ/mol			
80% crosslinked	42 kJ/mol			
60% crosslinked	41 kJ/mol			
40% crosslinked	41 kJ/mol			
Flexible resins				
100% crosslinked	53 kJ/mol	100%	70 kJ/mol	32 kJ/mol
80% crosslinked	52 kJ/mol	75%	53 kJ/mol	28 kJ/mol
60% crosslinked	55 kJ/mol	0%	49 kJ/mol	23 kJ/mol
40% crosslinked	58 kJ/mol			
Extended resins				
100% crosslinked	49 kJ/mol			
60% crosslinked	53 kJ/mol			
Non-amine resins				
100% crosslinked	37 kJ/mol			
Extrarigid resins				
100% crosslinked	46 kJ/mol			
60% crosslinked	48 kJ/mol			

[a] Data taken from ref. 6.

low the glass transition. This is reminiscent of the dependence of the equilibrium uptake on V_0, the local-scale topology, and the insensitivity on both the total hole volume fraction and the bulk density. However, if extensive, large-scale motions are introduced by entrance into the rubbery state, transport is significantly enhanced. Otherwise, the extent of motion in the glassy state does not affect the kinetics of transport.

Diffusion is generally observed to be an Arrhenius-activated process, and the epoxies here appear to conform to this phenomenology. $\ln(D)$ versus $1/T$ reveals a linear dependence whose slope is proportional to the activation energy, E_d, of the diffusion process, as summarized in Table I. Activation energies range from 40 to 60 kJ/mol, and within each resin series (rigid, flexible, etc.), negligible variation is encountered with crosslink density. For comparison, Table I also lists the β-relaxation activation energies obtained from dynamic mechanical measurements by Cukierman et al.[6] for the rigid and flexible resins. Two variations of the dynamic mechanical activation energy are reported: the traditional $E_{\alpha\text{-peak}}$ and $E_{\alpha\text{-onset}}$. These arise from performing time–temperature superposition relative to the peak (maximum loss) and onset regions of the β-relaxation peak. $E_{\alpha\text{-peak}}$ is significantly diminished with a decrease in crosslink density, whereas $E_{\alpha\text{-onset}}$, like E_d, remains constant. Furthermore, in the high crosslink density samples, the magnitude of $E_{\alpha\text{-peak}}$ exceeds E_d, whereas $E_{\alpha\text{-onset}}$ is of an appropriate magnitude (slightly smaller than E_d) to have an influence on transport; if $E_{\alpha\text{-peak}}$ were coupled to the diffusion process, one would not anticipate $E_{\alpha\text{-peak}}$ in the dry resin to be larger than E_d. We return to this issue of the magnitude of the activation energies in a more quantitative fashion once the role of the polar interactions is discussed. The most salient observation from this discussion is that the diffusion process is insensitive to large-scale cooperative motions of the glassy state and can only feel the local environment.

Influence of Polarity

The discussion of the previous section suggests the local molecular motions of the β-relaxation process determine the kinetics of transport. How-

ever, this implication is not entirely correct. Thus far, the kinetics of the non-amine resins have been overlooked. As shown in Figure 5(b) in the preceding publication,[3] at 5 °C the diffusion coefficients of the non-amine resins are one order of magnitude greater than the amine-containing resins. However, anhydride-cured resins, such as the non-amine resins, also exhibit a β-relaxation onset similar to the amine-containing resins.[12,13] Such an observation appears at odds with ascribing the transport kinetics to the local-scale motions of the β process. To resolve this apparent contradiction, one must consider the role of polarity. In the first publication,[2] the influence of polarity and topology on the equilibrium uptake are examined. At this point, it is beneficial to briefly reiterate a few important aspects of this previous article.

Resin polarity is of primary importance in determining the equilibrium moisture uptake. Less polar resins, such as the non-amine series, absorb very little water compared to the amine-containing materials. Accompanying polarity, topology has a secondary effect on uptake. A greater intrinsic hole volume fraction (V_0) leads to an increase in the equilibrium moisture content. V_0 is isothermally elevated by increasing crosslink density, the consequence of which is enhancement of the effective polarity. Steric hindrances at the crosslink junctions introduce unoccupied volume elements coincident with the polar hydroxyls and amines. This opens the matrix and facilitates access to and the association of water molecules with the polar groups, thus increasing the uptake. Returning to the discussion of kinetics, one must be cognizant of these water–epoxy interactions.

The polar sites adjacent to the crosslink junctions provide potential energy wells, or trapping sites, for a water molecule diffusing through the epoxy. The coincidence of the polar and unoccupied volume elements makes these epoxy–water interactions favorable from both an energetic and steric point of view. This trapping mechanism is effective at low temperatures as the diffusivity in the low-polarity non-amine resins is nearly an order of magnitude greater than in any of the highly polar amine-containing formulations (see Figure 5b of ref. 2). However, as the temperature increases, the trapping sites of the amine-cured resins become less attractive to the increasingly energetic water molecules, and the diffusion coefficients of the amine-containing and non-amine resins become similar. Figure 2 illustrates the differences in the potential energy landscape that a water molecule will encounter in an amine- and anhydride-cured epoxy. The average thermal energy of a water molecule as a function of temperature is indicated by the horizontal lines, depicting the decreased effectiveness of the potential wells at higher temperatures. The lack of trapping sites in the non-amine resins is similarly reflected in the lower activation energies of diffusion reported in Table I.

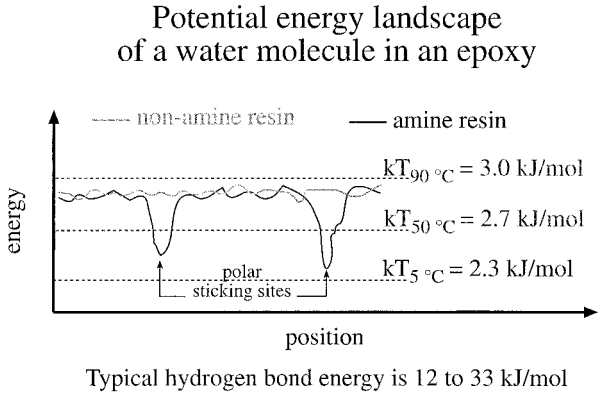

Figure 2. The differences in the potential energy landscape that a water molecule encounters in amine- and non-amine-cured epoxies. The polar sites in the amine resin provide potential energy wells that become less effective as traps when the kinetic energy of the water increases.

When the difunctional epoxies (rigid, semirigid, and flexible resins, two hydroxyls created per epoxy monomer) are used as a baseline, decreasing the polarity (non-amine resins, no hydroxyls created per epoxy monomer) increases the diffusion coefficient. However, increasing the polarity (extrarigid resins, three hydroxyls created per epoxy monomer) in the trifunctional epoxies does not decrease the diffusion coefficient. It is tempting to argue that this limitation is due to the topology controlling the number of polar sites effectively visible to water. Water can only interact with those polar groups it can access. However, the extrarigid resins do absorb significantly more water (see Fig. 4 of the original publication[2]), implying water can access a greater number of polar sites. In this respect, such a conclusion could be fortuitous; why the diffusion coefficient does not decrease with the added polarity is not immediately evident.

Combined Influence of Polarity and Molecular Motions

Thus far, two very different pictures of the diffusion process are presented: one emphasizing the

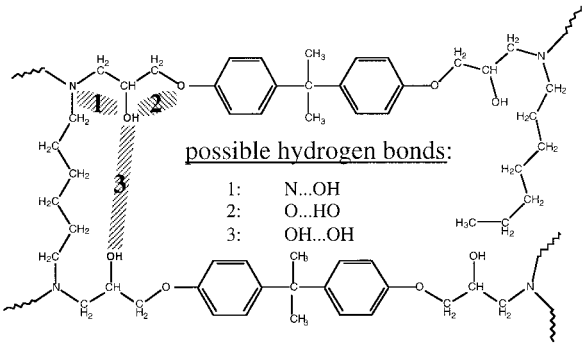

Figure 3. Three possible types of hydrogen bonds involving the hydroxyl of an amine-cured epoxy. Although the bonds are shown in the intramolecular sense (between covalent nearest neighbors), intermolecular analogues between nonbonded pairs are also possible.

molecular motions of the glassy state and the other the combination of polarity and openness. However, the two effects are not independent of each other, as is illustrated with infrared, dielectric, and NMR spectroscopy. Infrared spectroscopy is used by various researchers[19,20] to monitor hydroxyl bond stretching, which is indicative of the state of hydrogen bonding in the network. These works suggest that extensive hydrogen bonding exists in the typical epoxy network, persisting above the T_g and up to the point of thermal decomposition. The absorption for free hydroxyl stretching exhibits a peak at 3600 cm^{-1}, although epoxies rarely exhibit such a peak. These vibrations are hindered by the formation of hydrogen bonds, resulting in an absorbance peak in the 3600–3200 cm^{-1} range.[19,20] The exact nature of the hydrogen bonding is very complex and depends on factors such as the nucleophilicity of the amines, the distances between the polar species, and the presence of steric hindrances.

Three possible hydrogen-bond configurations are identified in Figure 3, as illustrated with a flexible resin. Configuration N. . .HO is an intramolecular bond in which the hydrogen from the hydroxyl extends back and couples with the tertiary amine at the crosslink junction. Considering acid–base interactions alone, this pairing should result in the strongest bond. The O. . .HO configuration is also an intramolecular hydrogen bond between the hydroxyl hydrogen and the closest ether oxygen. The third possibility is an OH. . .OH hydrogen bond between two hydroxyls. Evidence for each of these bonds exists,[19,20] although it is difficult to ascertain the relative extent to which each type will be present. Although the bonds are illustrated here in the intramolecular sense (between covalent closest pairs), it is possible for similar bonds to occur between nonbonded neighbors, creating a more intermolecular hydrogen bond (although in the strict sense a distinction between intramolecular and intermolecular is ambiguous in a crosslinked network). Regardless of the exact nature of the bonds, it is sufficient to note the hydroxyl group is involved in hydrogen bonding, even in the dry resins.

As seen with the uptake data,[2] there is evidence suggesting that sorbed water associates with the polar hydroxyl groups. This assertion is further supported by infrared,[21] dielectric,[22,23] and NMR spectroscopy[24] measurements. This information must be incorporated into the molecular picture being developed. The creation of a crosslink results in a local-scale increase in the unoccupied volume, coincident with the location of the hydroxyls and amines. The hydroxyls are extensively involved in hydrogen bonding with either the native polar species of the network or the foreign sorbed water molecules.

Solid-state NMR completes the picture of how polarity, topology, and molecular motions integrally influence transport. Two research groups examined similar epoxies using solid-state NMR, furnishing invaluable insight into specific molecular motions of the glassy state. Halary and Monnerie[8,25] extensively investigated the flexible resin series using both solid-state NMR and dynamic mechanical analysis. Although the true molecular underpinnings of the β-relaxation process remain ambiguous, it is evident that on activation of this process, the methylene groups in the —CH_2—CHOH—CH_2—O— and —CH_2—N— segments of Figure 3 could undergo rapid trans-gauche isomerizations. The timescale of these motions is approximately 1—10 kHz or faster. Similarly, Shi et al.[26] examined selectively deuterated versions of the rigid resins and confirmed the motions of the aforementioned methylenes on a similar timescale. Both groups observe coincident π flips of the bisphenol A phenyl rings on a timescale approximately one order of magnitude faster than the —CH_2—CHOH—CH_2—O— and —CH_2—N— motions. However, it is doubtful that π flips alone can account for the β relaxation because epoxies where such motions are impossible (e.g., epoxies with a locked ring structure[14] or epoxies based on an asymmetric 1,3 substitution of the phenyl rings as opposed to the symmetric 1,4 substitution of the DGEBA[8]) still exhibit sim-

Table II. Frequency of the Methylene Motions and π Flips of the Phenyl Rings in the 100% Crosslinked Rigid Resin Compared to the Average Jump Frequency (Γ) of the Diffusing Water Molecules

Temperature (°C)	$2\pi/\tau_p$-Methylenes (Hz)[a]	$2\pi/\tau_p$–π Flips (Hz)[a]	Γ (Hz)
5	0.13×10^5 [b]	1.9×10^5 [b]	1.5×10^5
35	1.3×10^5	15×10^5	12×10^5
50	1.9×10^5	35×10^5	32×10^5
70	4.4×10^5	94×10^5	76×10^5
90	6.3×10^5	217×10^5	135×10^5

[a] Data taken from ref. 26.
[b] Data taken at 0 °C (not at 5 °C as indicated).

ilar β-relaxation behavior. Regardless of the true foundations for the β relaxation, the —CH_2—CHOH—CH_2—O— and —CH_2—N— segments contain the polar amines and hydroxyls and are mobile. Further corroborating these motions, dielectric spectroscopy measurements in tetrafunctional epoxy cured with the diamino diphenyl sulfone detect a relaxation mechanism at 10 kHz associated with the reorientation of the hydroxyl group at the crosslink junction.[23] The intramolecular hydrogen bonds depicted in Figure 3 can only occur in a limited number of configurations. Motions of the hydroxyl groups will disturb any associations, potentially turning on and off the internal hydrogen bonds.

If a hydroxyl is involved in one of the aforementioned hydrogen bonds, it is unlikely that a water molecule can access the potential interaction sites. However, both NMR and dielectric spectroscopy indicate that the hydroxyls are mobile and that approximately every 10^{-4} s (2π/10 kHz) on average the water will have a chance to interact. Hayward et al.[23] confirmed this notion by demonstrating that the majority of the absorbed water has a relaxation frequency of $\sim 10^4$ Hz that is governed by the intramolecular potential between the hydroxyl and water and not by the mass of the water. The motions of the —CH_2—CHOH—CH_2—O— and —CH_2—N— segments, coincident with the activation of the β-relaxation process, control the association of water with the epoxy and, thus, the kinetics of transport.

In the NMR work of Shi et al.,[26] the forms of the deuterium solid-state echo delay line shapes as a function of varying delay times are used to determine the characteristic relaxation time, τ_p (in a Kohlrausch–Williams–Watts-stretched exponential, $\phi(t) = \exp[(-t/\tau_p)^\alpha]$), for the methylene motions. The inverse of τ_p provides an estimate of the frequency of these motions, as displayed in Table II. Between 0 and 90 °C (roughly the same temperature range as used for our diffusion measurements), the methylene transgauche isomerizations in the aforementioned segments occur in the frequency range of $\sim$ 10 to 100 kHz, with the higher frequencies occurring at the higher temperatures. This timescale can also be observed in the diffusion experiments, as is demonstrated next.

In the original publication,[2] the PALS hole volume fraction and average nanopore radius are used to estimate the number of nanopores per cubic centimeter. This estimation is repeated here for the specific example of the 60% crosslinked rigid resin, which has an average nanopore radius of 2.68 Å (slightly larger than a water molecule). Because water is a polar molecule, there are both geometric and energetic reasons for water to take up residence in the unoccupied volume elements. At 50 °C, the 60% crosslinked rigid resin has an absolute total hole volume fraction of 3.87%. Given the density of this material, there are approximately 5×10^{20} nanopores per cm^3. Similar estimations suggest there are approximately 2×10^{21} hydroxyl groups per cm^3. The equilibrium uptake is 2.15 wt %, which corresponds to an absorption of 9×10^{20} water molecules per cm^3. Although such estimations are crude, the number of polar sites, nanopores, and water molecules appear to agree within an order of magnitude. These calculations should not be taken as direct evidence or support for a one-to-one correlation between the polar sites, nanopores, and sorbed water molecules. Rather, they simply suggest that the concept of the nanopores being localized adjacent to the crosslink junctions, and thus in association with hydroxyls, appears reasonable.

This approximation can be elaborated by the assumption that the nanopores are distributed in a simple cubic array. With this arrangement, the

average distance between the nanopore centers, ζ, is determined to be 12–13 Å for the 60% crosslinked rigid resin (as well as all crosslink densities of the rigid resins). Examination of the chemical structure of the rigid resin suggests that 12–13 Å is a reasonable approximation for the distance between the crosslink junctions. This is also consistent with the previous assertion of the nanopores being coincident with the crosslink junctions. If water diffuses through the nanopores from polar site to polar site, it is reasonable to expect the average diffusive jump length to correlate with the distance between nanopores or junctions. Using an atomic equation of diffusion, one can relate the diffusion coefficients to a jump frequency, Γ, if the jump length, l, is known through the relationship:

$$D = (1/6)l^2\Gamma \quad (1)$$

By setting l equal to ζ and using D from the absorption experiments, one can estimate the jump frequency. The resulting jump frequencies as a function of temperature for the 100% rigid resin are given in Table II. The jump frequencies appear to be well within an order of magnitude of the molecular motions measured by solid-state NMR (and dielectric spectroscopy). Given the simplistic nature of this estimation, the reasonable agreement further suggests that the local motions of polar segments regulate the association of water with the polar sites and, thus, govern the kinetics of transport.

The final argument for the concerted efforts of the specific hydrogen bonds and the molecular motions governing the transport process comes from the activation energies. Generally, hydrogen bonds have bond energies in the range of 10–30 kJ/mol. Table I reports that the activation energy for the onset of the β relaxation, which previously has been argued to govern the kinetics of transport, is approximately 20–30 kJ/mol. If the 10–30 kJ/mol necessary to overcome the hydrogen bonds is added to this onset activation energy, the resulting value is very consistent with the observed 40–60 kJ/mol activation energies of the diffusion process. Granted, a simple addition of the two processes is debatable. However, the approximate nature of the results suggests that the physics of this discussion is not too far off.

Nature of the Nanopores

Before a discussion of the physical meaning of the nanopores, it is crucial realize that a water molecule, with a kinetic radius of 1.3 Å, should be able to traverse the regions of unoccupied volume. In fact, it is likely that these nanopores form interconnected pathways of unoccupied volume with respect to a penetrant the size of a water molecule. Recent molecular dynamics simulations by Greenfield and Theodorou[27,28] support this assertion. In their simulations, a random atomic glass (no covalent bonds) is formed from united atoms representing the methyl, methylene, and methyline groups (they all have a radius of approximately 2 Å) of poly(propylene) (PP). A theoretical penetrant molecule is introduced into the unoccupied regions of the resulting atomic glass, and the penetrant radius is adjusted until the critical radius for percolation is attained. For the random atomic glass, the critical radius is 0.5 Å. Next, the united atoms of the simulation are polymerized into a linear, atactic PP structure. The prescribed bond angles and lengths reduce the packing efficiency and increase the critical radius for percolation from 0.5 to 0.9 Å. Similar simulations have not been done on epoxy networks where the chains are connected in three dimensions, not two dimensions (like linear PP). However, one logically would expect the more restricted epoxy networks to exhibit an even larger critical radius for percolation. Given the current trend, it is very plausible that a water molecule with a kinetic radius of 1.3 Å will encounter interconnected regions of unoccupied volume.

The idea of interconnected nanopores is consistent with structural simulations of poly(carbonate) by Gusev et al.[29] [both poly(carbonate) and our DGEBA epoxy are based on the rigid bisphenol A moiety]. They reported pores of accessible volume approximately 5–10 Å in diameter connected by bottlenecks or channels that were 1–2 Å in diameter and 5–10 Å in length. Granted, such computer simulations are challenged to capture the long time dynamics of a polymer network. However, they should provide a reasonable snapshot of the pore structure. Dynamic mechanical, dielectric, and NMR spectroscopy measurements clearly indicate the presence of molecular motions occurring on a timescale greater than those accessible with the molecular dynamics simulations. In the picture here, we envision the interconnected pathways of open volume to be dynamic or transient in nature. Both local- and large-scale motions exist in the glass, and these larger scale motions should impart a breathing motion to the nanopore structure. However, the dynamic mechanical spectra suggest that the diffusion of wa-

ter is not extremely sensitive to these larger scale motions.

This latest picture is somewhat disturbing in light of the previous discussions on the nanopores in terms of spherical voids. Clearly, there is no physical reason for the nanovoids to be spherical; a tortuous, tubelike geometry is perhaps more intuitive. This brings into question the analysis of the preceding sections where the nanopores are assumed to be spherical. We must address the question of how nonspherical nanovoids affect the analysis. The issue has been scrutinized in the past with both experiment and theory. First, Jean and Shi[30] looked at positronium annihilation in elliptical nanopores. They found that the lifetime was dominated by the shorter, or minor, dimension of the ellipse. Consistent with these experiments, Xie[31] solved the quantum mechanical probabilities for ortho-positronium pick-off annihilation in potential energy wells bound by either infinite parallel plates or an infinite tube. In each case, the lifetime was dominated by (slightly larger than indicated by) the shorter dimension, which could be either the separation of the plates or the diameter of the tube. Returning to the discussion of the dynamic, channel-like pores, one should regard τ_3, and the corresponding radius to be indicative of an average tube radius. Unfortunately, τ_3 does not convey information about the length of the tubes.

As we look back at the moisture-transport properties presented in the previous two articles, several observations appear to make more sense in terms of a continuous nanopore network. First, if water were to hop from isolated nanopore to nanopore, increasing the nanopore volume fraction would decrease the distance between the nanopores. A decreased nanopore separation would decrease the energy barrier to such a hopping mechanism and, thus, increase the diffusion coefficient. However, the diffusion coefficient does not vary significantly with the nanopore size or volume fraction. Although the spherical nanopore concept has difficulties explaining this phenomena, the results are easily rationalized in the framework of a continuous nanopore network.

In the earlier publication,[2] the effects of physical aging on the transport behavior are also discussed. Depending on the depth into the glassy state of the material, aging can significantly impede transport and retard the moisture uptake. Physical aging is known to densify the resin, and in this case, the density increased on average by ~0.25%. Although it was not mentioned in the previous publication (see ref. 32 for the experimental data), physical aging does not produce a measurable change in the size or volume fraction of nanopores. This too can be rationalized in terms of a long tubelike network of nanopores. The crosslink junctions clearly are vital for establishing the nanopore networks. The steric restrictions at the crosslink junction cause the packing to suffer and increase the openness. Pure physical aging does not alter these covalent crosslinks, and the nanopores remain open locally. However, away from the crosslink sites, the degrees of freedom are greater, and the structure can relax during the aging process. In terms of the tubelike voids, in the regions immediately adjacent to the crosslink, the nanovoids are propped open by the covalent restrictions. However, away from the junction, the tubelike void is pinched off to some extent by the relaxing matrix. This pinching off could impede moisture transport through the nanopore networks. In PALS, the ortho-positronium quasiparticle always looks for the lowest electron density regions in which to localize. If the choice of localizing in a pinched-off portion of the void or a propped-open section near the junction is given, the more open location will be preferred. This might explain why the numbers of nanopores, water molecules, and polar groups are within an order-of-magnitude agreement. This might also describe why the PALS technique is not sensitive to physical aging, whereas moisture diffusion is. Another way to probe this idea would be to study samples with a slightly larger penetrant molecule that would be sensitive to the size of the nanopores.

Obviously, this latest revelation on the nanopore geometry places uncertainty on the volume fraction of nanopores calculated and used frequently in our previous two publications[2,3] on these materials. These volume fractions were calculated under the spherical nanopore assumption. In this respect, they should be taken at face value, an estimation of the nanoscale porosity using the spherical nanovoid assumption. Despite the obvious limitation on this assumption, the estimations still provide insight into the topology of the glass.

Molecular Mechanisms of Transport

The preceding discussions are now summarized in terms of a reasonable molecular picture of the transport process. Although some of the exact details of this molecular picture remain to be ver-

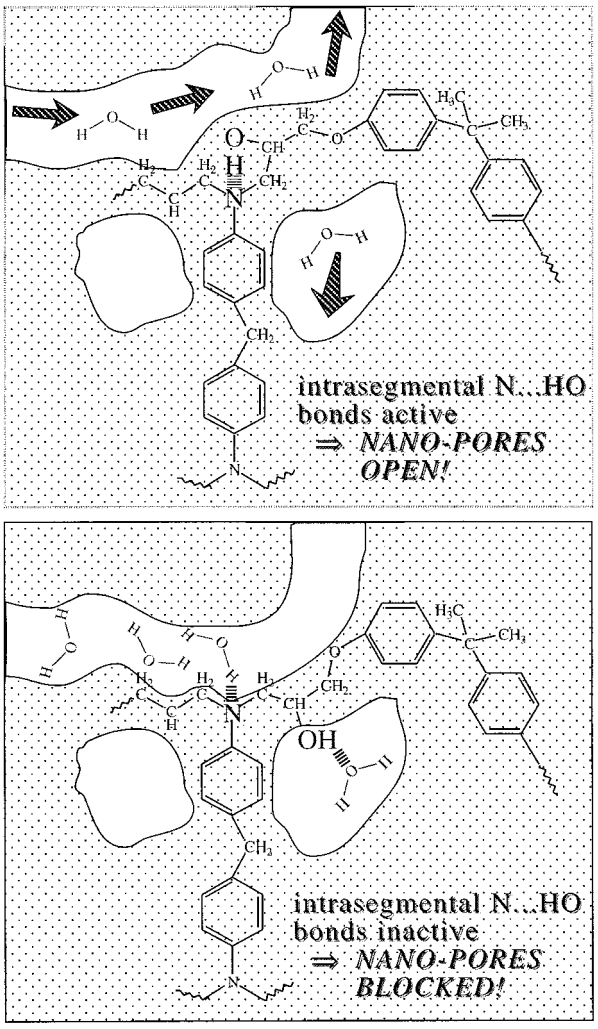

Figure 4. A plausible picture of moisture diffusion through the nanopores of an amine-containing epoxy resin where specific interactions between the water and the polar hydroxyls and amines regulate transport.

ified by direct experimental observation, we feel the discussion is useful because it emphasizes how topology, polarity/interactions, and molecular motions combine together to dictate the transport process.

Figure 4 illustrates the nanopores in a region adjacent to a crosslink junction. In accordance with the PALS data, the nanopores are drawn slightly larger than the water molecules. In the bottom portion of Figure 4, the intramolecular N. . .HO hydrogen bond is shown in the disrupted state, allowing water molecules to interact with the amine and the hydroxyl. This association momentarily blocks that particular nanopore and impedes transport. However, in the top half of Figure 4, the intramolecular N. . .HO bond is drawn in the bonded state, precluding a water molecule from associating with either polar group. The water molecules cannot associate with the shielded polar sites and, hence, can easily traverse the nanopores. In this model, the polar sites act as the bottleneck for transport through the nanopores, and the association/disassociation rate of the internal hydrogen bonds regulates the transport. In Figure 5, a similar representation is given for a non-amine resin, where the polar amines and hydroxyls are absent. In this case, transport proceeds relatively unhindered because of the absence of trapping sites, as reflected in the enhanced diffusion coefficients.

In the scope of this study, the nanopore structure does not significantly influence the transport kinetics. This is attributed to the dominating influence of the polar groups. One intuitively would expect the nanopore structure to influence transport as the nanopores are of a size similar to that of the water molecules. In the absence of trapping sites, it remains to be seen whether the nanopore volume correlates with the transport. With only one nonpolar resin included in this study, insufficient data exists to establish such correlations. An alternative approach would be to study the diffusion of a penetrant molecule that does not interact with the epoxy. However, nonpolar, noninteracting penetrants, of a size comparable to water, are gaseous, which makes weight-gain ex-

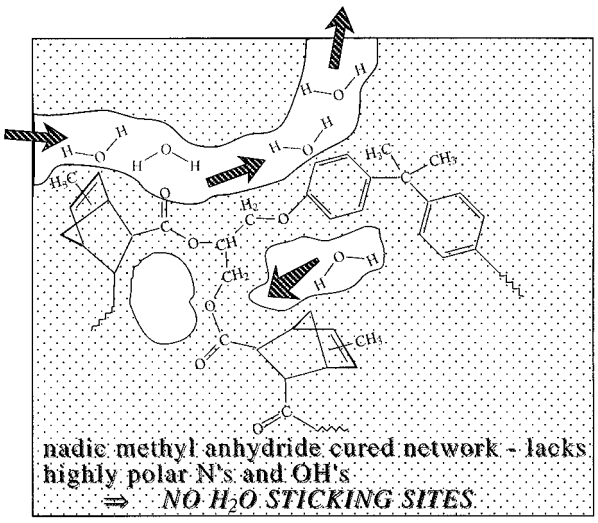

Figure 5. A plausible picture of moisture diffusion through the nanopores of the non-amine resins where the lack of polar trapping sites leads to an enhanced diffusion coefficient.

periments more difficult. Current efforts in our laboratory focus on understanding the role of topology and molecular motions in these noninteracting systems.

CONCLUSIONS

A discussion of the mechanisms of moisture transport in amine-cured epoxies is offered here to develop a plausible molecular picture of the diffusion process. In this description, the topology, polarity, and molecular motions combine to control transport. Water traverses the epoxy through the network of nanopores, which are also coincident with the polar hydroxyls and amines. In this respect, the nanopores provide access routes for the water to reach the specific interaction sites. The sub-T_g molecular motions associated with the onset of the β-relaxation process in an epoxy incorporate these interaction sites and, hence, regulate the association of water with the epoxy. In effect, the dynamics of the local-scale motions of the β-relaxation process dictate the kinetics of transport. The volume fraction of the nanopores does not appear to be a rate-limiting factor for the diffusion of water through an amine-cured epoxy.

The authors would like to thank the Air Force Office of Scientific Research for funding this research under Grant F-49620-95-1-0037. Furthermore, we appreciate the constructive criticism provided by Professors Richard Robertson, David Srolovitz, and David Gidley of the University of Michigan, Professor Andre Lee of Michigan State University, Professor Annelise Faivre of the Université Montpellier II, Dr. Brett Bolan, Dr. Hristo Hristov, and Mr. Fernando Chang.

REFERENCES AND NOTES

1. Halpin, J. P.; Pandolfini, P. P.; Biermann, P. J.; Kistenmacher, T. J.; Hunter, L. W.; O'Connor, J. S.; Jablonski, D. Johns Hopkins APL Tech Dig 1997, 18, 33.
2. Soles, C. L.; Chang, F. T.; Bolan, B. A.; Hristov, H. A.; Gidley, D. W.; Yee, A. F. J Polym Sci Part B: Polym Phys 1998, 36, 3035.
3. Soles, C. L.; Chang, F. T.; Gidley, D. W.; Yee, A. F. Polym Sci Part B: Polym Phys 2000, 38.
4. Kumins, C. A.; Kwei, T. K. In Diffusion in Polymers; Crank, J.; Park, G. S., Eds.; Academic: London, 1968; Chapter 4.
5. Cukierman, S.; Halary, J.-L.; Monnerie, L. J Non-Cryst Solids 1991, 131–133, 898.
6. Cukierman, S.; Halary, J.-L.; Monnerie, L. Polym Eng Sci 1991, 31, 1476.
7. Gerard, J. F.; Galy, J.; Pascault, J. P.; Cukierman, S.; Halary, J.-L. Polym Eng Sci 1991, 31, 615.
8. Heux, L.; Halary, J.-L.; Lauprêtre, F.; Monnerie, L. Polymer 1997, 38, 1767.
9. Heux, L.; Halary, J.-L.; Lauprêtre, F.; Monnerie, L. Polymer 1998, 39, 1269.
10. Pogany, G. A. Polymer 1970, 11, 66.
11. Williams, J. G. J Appl Polym Sci 1979, 23, 3433.
12. Takahama, T.; Geil, P. H. J Polym Sci Polym Phys Ed 1982, 20, 1979.
13. Ochi, M.; Iesako, H.; Shimbo, M. J Polym Sci Polym Phys Ed 1986, 24, 1271.
14. Ochi, M.; Yoshizumi, M.; Shimbo, M. J Polym Sci Polym Phys Ed 1987, 25, 1817.
15. Charlesworth, J. M. Polym Eng Sci 1988, 28, 221.
16. Starkweather, H. W. J. Macromolecules 1981, 14, 1277.
17. Starkweather, H. W. J. Macromolecules 1986, 19, 2541.
18. Starkweather, H. W. J. Macromolecules 1988, 21, 1798.
19. Williams, J. G.; Delatycki, O. J Polym Sci A2 1970, 8, 295.
20. Bellenger, V.; Verdu, J.; Francillette, J.; Hoarau, P.; Morel, E. Polymer 1987, 28, 1079.
21. Netravali, A. N.; Fornes, R. E.; Gilbert, R. D.; Memory, J. D. J Appl Polym Sci 1984, 29, 311.
22. Maxwell, I. D.; Pethrick, R. A. J Appl Polym Sci 1983, 28, 2363.
23. Hayward, D.; Hollins, E.; Johncock, P.; McEwans, I.; Pethrick, R. A.; Pollock, E. Polymer 1997, 38, 1151.
24. Fuller, R. T.; Sherrow, S.; Fornes, R. E.; Memory, J. D. J Appl Polym Sci 1979, 23, 1383.
25. Lauprêtre, F.; Estache, R.-P.; Monnerie, L. Polymer 1995, 36, 267.
26. Shi, J.-F.; Inglefield, P. T.; Jones, A. A.; Meadows, M. D. Macromolecules 1996, 29, 605.
27. Greenfield, M. L.; Theodorou, D. N. Macromolecules 1993, 26, 5461.
28. Theodorou, D. N. In Diffusion in Polymers; Neogi, P., Ed.; Marcel Dekker: New York, 1996; Chapter 2.
29. Gusev, A. A.; Arizzi, S.; Suter, U. W. J Chem Phys 1993, 99, 2221.
30. Jean, Y. C.; Shi, H. J. Non-Cryst Solids 1994, 172–174, 806.
31. Xie, L. Ph.D. Thesis, University of Michigan, 1995.
32. Soles, C. L. Ph.D. Thesis, University of Michigan, 1998.